International Journal of Bifurcation and Chaos, Vol. 21, No. 8 (2011) 2305–2319

DOI: 10.1142/S021812741102980X

SUBCRITICAL PATTERN FORMATION IN GRANULAR FLOW

GIORGOS KANELLOPOULOS* and KO VAN DER WEELE†
Department of Mathematics,
Center for Research and Applications of Nonlinear Systems,
University of Patras, 26500 Rio Patras, Greece
**kanellop@master.math.upatras.gr*
†*weele@math.upatras.gr*

Received December 24, 2010; Revised April 8, 2011

We study a minimal model for the flow of granular material on a conveyor belt consisting of a staircase-like array of K vertically vibrated compartments. Applying a steady inflow rate Q to the top compartment, we determine the maximum value $Q_{\rm cr}(K)$ for which a continuous flow through the system is possible. Beyond $Q_{\rm cr}(K)$, which depends on the vibration strength and the dimensions of the system, a dense cluster forms in one of the first compartments and obstructs the flow. We find that the formation of this cluster is already announced *below* $Q_{\rm cr}(K)$ by the appearance of an oscillatory density profile along the entire length of the conveyor belt, with a distinct two-compartment wavelength.

These model predictions concerning the breakdown of the granular flow admit an elegant explanation in terms of bifurcation theory. In particular, the subcritical oscillatory pattern is shown to be a side effect of the period doubling bifurcation by which the uniform density profile (associated with a smooth particle flow) becomes unstable. The effect turns out to be robust enough to survive the presence of a reasonable amount of noise and even certain qualitative modifications to the flux model. The density oscillations may therefore well be of practical value and provide a warning signal for imminent clustering on actual conveyor belts.

Keywords: Granular flow; clustering; subcritical pattern formation.

1. Introduction

One of the major problems with the transport of granular matter — encountered in numerous industries worldwide — is the formation of dense particle clusters that impede the flow. This happens due to the inelasticity of the particle collisions [Goldhirsch & Zanetti, 1993; Jaeger *et al.*, 1996; Kudrolli *et al.*, 1997]. In every collision, the particles lose a portion of their kinetic energy and hence they tend to slow each other down. This leads to the formation of clusters in regions where there is a slight surplus of particles, at the cost of emptying the other, more dilute areas. Such regions of slightly higher density will always appear, even in the absence of human intervention, due to statistical fluctuations.

Here we study this phenomenon in the model transport system shown in Fig. 1, consisting of K connected compartments in a staircase-like array, vertically vibrated with a tunable amplitude and frequency. Given a certain inflow rate of particles into the top compartment ($F_{\rm in}$) and applying a box-to-box flux function (defined in Sec. 2), we measure the outflow $F_R(n_K)$ from the bottom compartment.[1] Under steady operating conditions

[1]Note that the system described here represents, in an idealized way, just one of the many types of compartmentalized transport devices used in industry and agriculture. Often one also encounters conveyor belts that carry the material upwards instead of downwards, or with the compartments not placed in a straight line but e.g. in a helix [Evesque, 1992].

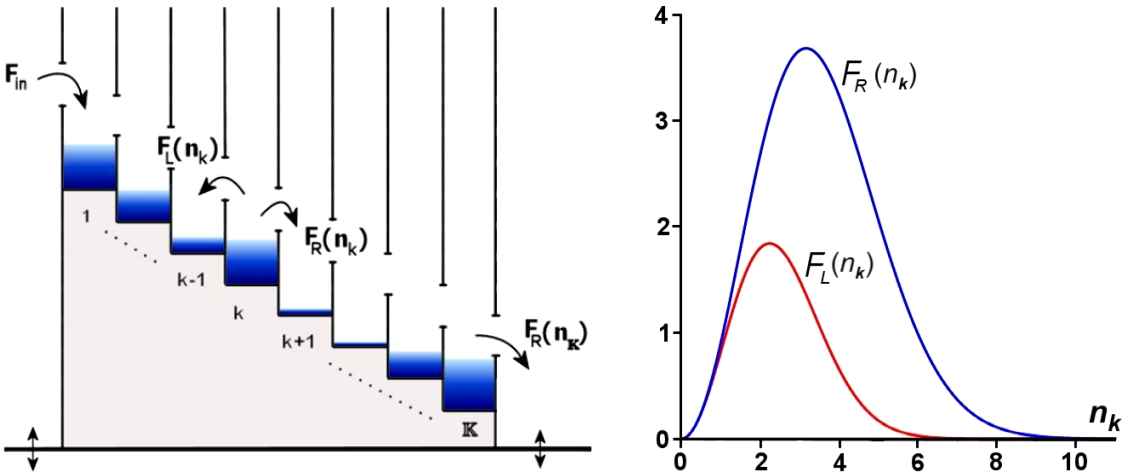

(a) (b)

Fig. 1. (a) Sketch of the conveyor belt, consisting of K connected compartments, vertically vibrated to make the granular particles mobile. The adjustable inflow rate into the top compartment is denoted by $F_{\rm in}$ and the outflow rate from the rightmost compartment by $F_R(n_K)$. (b) The flux functions $F_R(n_k)$ and $F_L(n_k)$, which model the particle flow from compartment k to its neighbors at the right- and left-hand sides, respectively.

the outflow is equal to the inflow. For reasons of efficiency, one usually wants the outflow to be as large as possible, so we will pay particular attention to this optimal case.

This optimum happens to be *critical* in the sense that as soon as the inflow rate exceeds the maximum capacity of the system, the densities become locally so high that clustering sets in. Fortunately, as we will see, the cluster formation is announced already below the critical value of $F_{\rm in}$ by the appearance of an oscillatory density profile. In practical applications this may serve to warn the operator of the conveyor belt that the maximum capacity has almost been reached. The oscillations signal that the inflow rate must not be increased any further. Actually, it would be advisable to decrease it a bit, to guarantee a regular flow also in the unavoidable presence of fluctuations.

The oscillatory density profile is not only of great potential benefit for industries, it is also a prime example of spontaneous pattern formation in a dynamical system far from equilibrium. The input of energy on the one hand (via the vibrating bottom, as well as via the gain in kinetic energy every time a particle jumps towards a lower compartment) and the dissipation on the other hand (via the nonelastic particle collisions) make this an open energy system. It is also open with respect to mass, due to the in- and outflow of particles. This means that the conveyor belt of Fig. 1 is a system inherently out-of-equilibrium, continuously exchanging energy and matter with the outside world, and that pattern formation can occur without violating the second law of thermodynamics [Cross & Hohenberg, 1993].

2. Flux Model

The flow from compartment to compartment will be modeled by a flux function [Eggers, 1999; Van der Weele *et al.*, 2001; Van der Weele *et al.*, 2004; Van der Meer *et al.*, 2007; Van der Weele, 2008; Kanellopoulos & Van der Weele, 2008; Van der Weele *et al.*, 2009]:

$$F_{R,L}(n_k) = An_k^2 e^{-B_{R,L}n_k^2}, \tag{1}$$

which gives the flow of particles per unit time from compartment k, to the right (R) and left (L), respectively. Here $n_k(t)$ represents the dimensionless particle content of the kth compartment at time t. It is the number of particles in compartment k normalized in such a way that initially (at $t = 0\,$s) the total particle content of the system is $\sum_{k=1}^{K} n_k(0) = C$, with C a non-negative constant. So the average value of the initial quantities $n_k(0)$ is C/K (which, if so desired, may be set to 1 by choosing C equal to the total number of compartments K). We will treat the quantity $n_k(t)$ as a continuous variable, implying that the granular material in our approach is modeled as a continuous medium. This is a good approximation as long as there are sufficiently many particles in each compartment.

The flux function $F(n_k)$ given in Eq. (1) is essentially identical to that derived by Eggers on

the basis of granular hydrodynamics under several simplifying assumptions [Eggers, 1999] (see also [Van der Meer *et al.*, 2007] and [Van der Weele, 2008] for further details). For example, the particle-wall collisions are assumed to be perfectly elastic and the equation of state (relating the pressure p, the particle density in each box, and the granular temperature T) is taken to be the ideal-gas law. The simplifying assumptions can in principle all be refined by taking higher order approximations. In the present paper, however, we choose to work with the "minimal" model, in the sense of Occam's razor, in order to unravel the bare essentials of the breakdown of the particle flow. In Sec. 5.2, we will come back to this and discuss a modified form of the flux function (which may more accurately mimic the behavior of the granular particles) and test to what extent the results obtained from Eggers' model survive the modification.

The factor A, which has dimensions $\sec^{-1}$, sets the time scale of the flow and will be used to nondimensionalize the time variable (this is equivalent to taking $A = 1\,\sec^{-1}$ throughout).

The dimensionless parameter $B_{R,L}$ is proportional to

$$B_{R,L} \propto \frac{g h_{R,L}}{(af)^2}\varepsilon^2, \tag{2}$$

where $g = 9.81\,\mathrm{m/sec}^2$ denotes the gravitational acceleration, $h_{R,L}$ the height of the barrier towards the neighboring compartment at the right and the left, respectively, a and f the amplitude and frequency of the sinusoidal driving signal, and ε the inelasticity parameter, which typically has a value of $\varepsilon = 0.10$. This inelasticity parameter is related to the well-known coefficient of normal restitution η of the particles via $\varepsilon = (1 - \eta^2)$. The value $\varepsilon = 0.10$ corresponds to spherical glass particles with a diameter of 2 mm, which have a restitution coefficient $\eta \approx 0.95$, quite close (but not equal) to the value $\eta = 1$ for completely elastic collisions.

The flux to the right $F_R(n_k)$ is considerably larger than the flux to the left $F_L(n_k)$ (see Fig. 1), owing to the fact that the height h_R is smaller than h_L. We will take $B_R = 0.1$ and $B_L = 0.2$, which means that h_R is twice as low as h_L.

The one-humped shape of the flux functions is directly related to the nonelasticity of the particle–particle collisions. For small values of n_k, the flux from compartment k grows with increasing density just as in a nondissipative fluid; beyond a certain value of n_k, however, the increasingly frequent collisions make the particles so slow that they are hardly able to overcome the barrier anymore, and hence the flux decreases. Naturally, the value of n_k at which the flux starts to decrease towards the *left*-hand side (with the high barrier) lies lower than that for the *right*-hand side. To be specific, the maxima lie at $n_k = 1/\sqrt{B_L} = 2.24$ and $n_k = 1/\sqrt{B_R} = 3.16$ respectively, cf. Fig. 1. Especially the latter value will play an important role in the clustering, as we will see later.

Given the above flux functions, and a controllable influx $F_{\mathrm{in}}(t)$ into the first compartment, the time evolution of the system is governed by the following system of K coupled ordinary differential equations:

$$\begin{aligned}
\frac{dn_1}{d\tau} &= F_{\mathrm{in}}(\tau) - F_R(n_1) + F_L(n_2), && \text{for compartment } k = 1,\\
\frac{dn_k}{d\tau} &= F_R(n_{k-1}) - F_L(n_k) - F_R(n_k) + F_L(n_{k+1}), && \text{for } k = 2, \ldots, K-1,\\
\frac{dn_K}{d\tau} &= F_R(n_{K-1}) - F_L(n_K) - F_R(n_K), && \text{for the last compartment } k = K,
\end{aligned} \tag{3}$$

where we have introduced the dimensionless time variable $\tau = At$, which means that the system is now fully nondimensional. These equations express the mass balance for each compartment k (and should thus be interpreted as the continuity equations for the system): The change in the density $n_k(\tau)$ per unit time is simply equal to the inflow rate into this compartment minus the outflow rate.

3. Observations Around the Critical Flow Rate

Let us consider the case with $K = 25$ compartments. We start with a uniform density profile $n_k(0) = 1$ for all $k = 1, \ldots, K$ and apply a constant inflow rate $F_{\mathrm{in}}(\tau) = Q$ into the first compartment. If the value of Q is sufficiently small

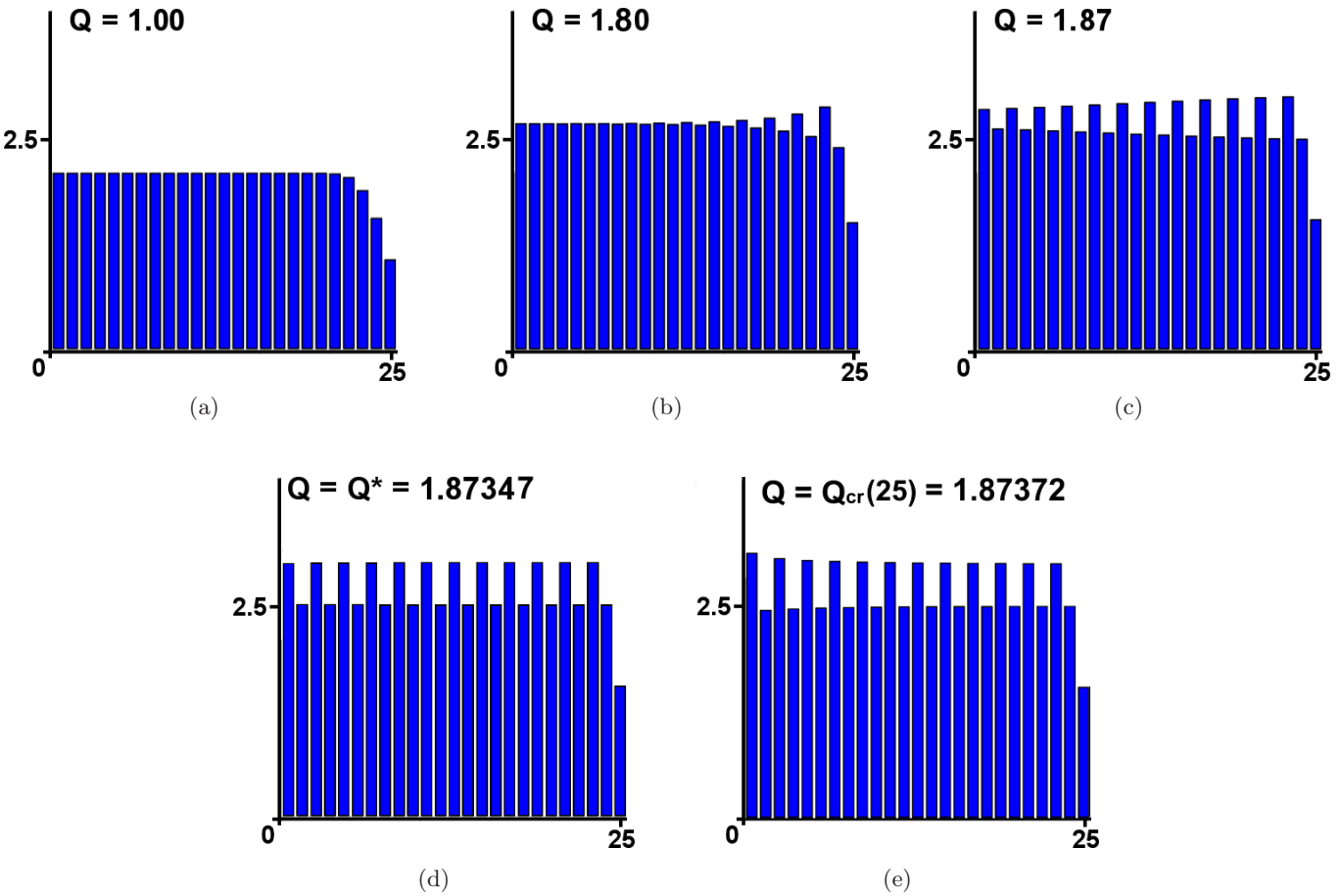

Fig. 2. (a) Starting from the equilibrium state at $Q = 1.00$ we gradually increase the inflow rate, in small steps, and after each step let the system adapt itself to the new Q-value. Each of the depicted density profiles thus represents a dynamical equilibrium in which the outflow (from the last compartment) equals the inflow (into the first compartment). (b) Already at $Q = 1.80$ the oscillatory profile appears on the right-hand side of the conveyor belt and (c) at $Q = 1.87$ the oscillatory pattern has spread over the entire system. (d) At $Q = Q^* = 1.87347$ the amplitude of the oscillations is precisely constant. (e) At the critical value $Q = Q_{\rm cr}(25) = 1.87372$ the system operates at its maximum capacity.

(i.e. well below the maximum capacity of the conveyor belt) the material will flow smoothly downward and after a while a dynamical equilibrium situation along the entire length of the system is reached. From that moment on the density profile does not change anymore. In Fig. 2(a), we show the equilibrium profile for $Q = 1.00$. The dimensionless density is uniform (slightly above 2) everywhere except at the very end of the system, where the density drops to the significantly lower value $n_K = 1.06$ of the last compartment. In the next section we will demonstrate how this value is evaluated.

Now, if we gradually increase Q, in small steps of Q and each time allowing the system to settle in its new equilibrium state, the density in the system rises steadily. At some point, however, the maximum capacity of the system will be reached and clustering becomes inevitable. This critical point (which lies at $Q_{\rm cr} = 1.87372$ for the present system with $K = 25$ compartments) is announced well in advance by the appearance of an oscillatory profile with a spatial periodicity of two compartments. Figures 2(b) and 2(c) show how the oscillatory profile is formed, emerging from the rightmost end of the conveyor belt and — for increasing Q — working its way upstream towards the first compartment. It is a beautiful example of *subcritical pattern formation*. At $Q = Q^* = 1.87347$ [Fig. 2(d)] the wavy profile becomes uniform along the whole length of the system, and at the critical value $Q = Q_{\rm cr}(25) = 1.87372$ [Fig. 2(e)] we observe a slight but distinct preference for the leftmost part of the system. The profile has in these final stages tilted from right to left and is now on the brink of collapsing.

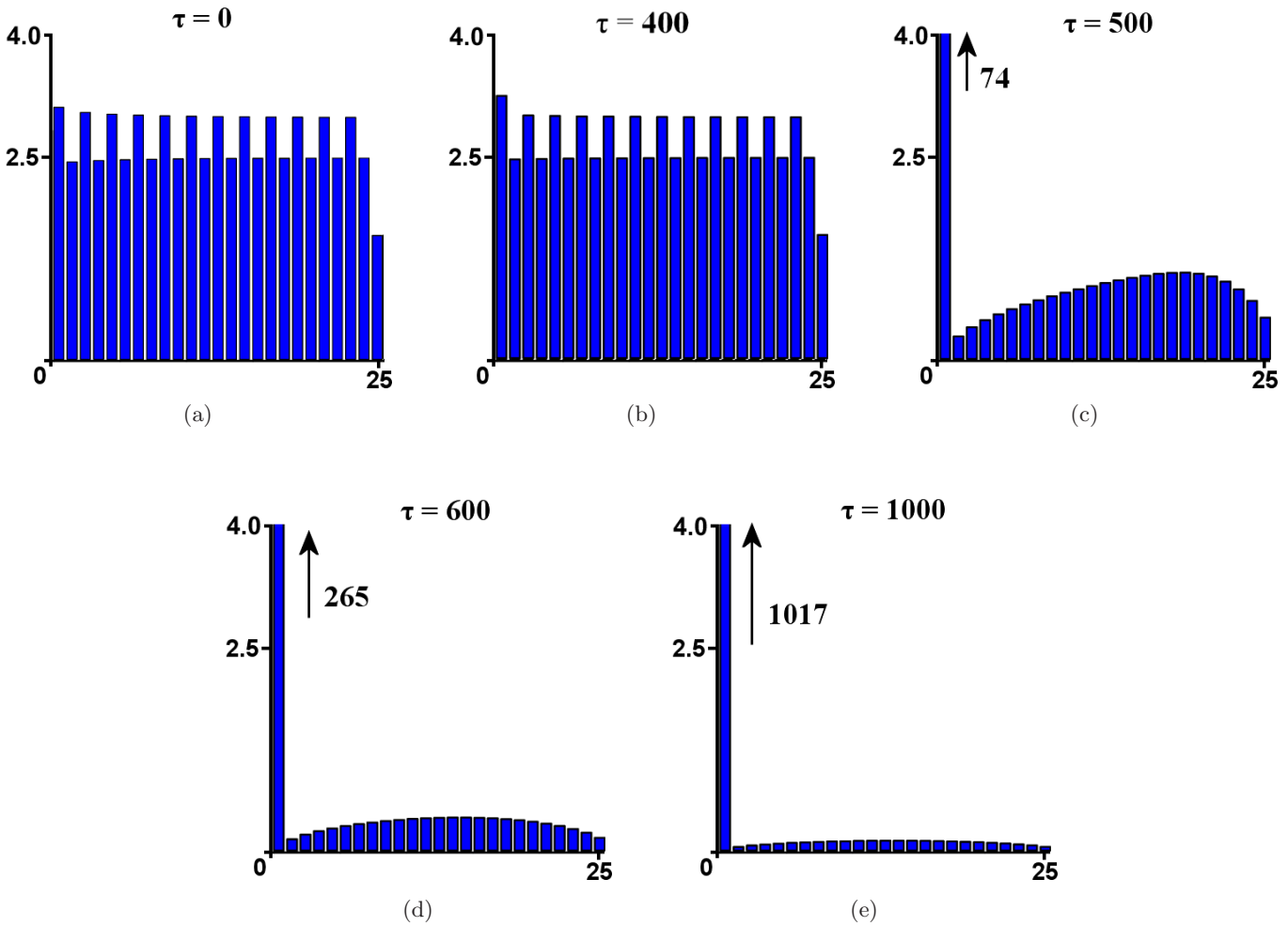

Fig. 3. Series of snapshots showing the breakdown of the steady flow. Starting from the critical profile of Fig. 2(e) and increasing the inflow just a little bit further, to $Q = 1.87400 > Q_{\rm cr}(25)$, we observe that a cluster is formed in the first compartment: all the incoming material is trapped here. The particles that were present in compartments $2, 3, \ldots, K$ still continue to flow to the right (and out of the system) but this outflow gradually comes to a halt.

In Fig. 3, we see what happens when we exceed the critical inflow rate. Here, at $Q = 1.87400 > Q_{\rm cr}(25)$, the flow breaks down because all the incoming material clusters in the first compartment. The particles that were present in the other compartments still flow out of the system, but in due time this outflow vanishes. It is interesting to see how the outflow of the remaining material first organizes itself in the form of a shock wave with a recognizable front (see the snapshot at $\tau = 500$). Later — when the compartments are sufficiently diluted — the density profile takes on a more symmetric shape, because in the limit $n_k(\tau) \to 0$ the flux functions $F_L(n_k)$ and $F_R(n_k)$ become identical, meaning that the material diffuses to both sides with the same ease [Van der Weele *et al.*, 2009].

4. Explanation of the Subcritical Density Oscillations

4.1. *Destabilization of the uniform flow*

To explain the appearance of the oscillatory profile, we start with a simple observation: An equilibrium flow through the system necessarily implies a local balance between any two neighboring compartments. In other words, the net flow per unit time through the opening between any two compartments must be equal to Q:

$$F_R(n_k) - F_L(n_{k+1}) = Q. \tag{4}$$

For the last compartment ($k = K$) this takes the form $F_R(n_K) = Q$, which simply states that under steady flow conditions the outflow from the

last box is equal to the influx into the first one. This uniquely determines the density $n_K(Q)$ at the very end of the conveyor belt. In fact, writing out the final-compartment balance as $n_K^2 e^{-B_R n_K^2} = Q$, we have an equation that admits an analytic solution:

$$n_K(Q) = \sqrt{-\frac{1}{B_R} W(-B_R Q)}, \tag{5}$$

where $W(x)$ is the LambertW function depicted in Fig. 4(a) [Corless *et al.*, 1996]. The solution (5) is shown in Fig. 4(b); as expected, it is a monotonically increasing function of the inflow rate Q. It grows from $n_K(Q) = 0$ at $Q = 0$ to $n_K(Q) = B_R^{-1/2} = 3.16$ at $Q = Q_{\max} = (eB_R)^{-1} = 3.67$ (for our choice of $B_R = 0.1$). This latter value corresponds to the density at which the flux function $F_R(n_k)$ attains its maximum, which is logical, since beyond this density, the outflow starts to decrease if one keeps adding more material; so the compartment gets blocked and the flow is halted.

Given the density of the last compartment, $n_K(Q)$, the densities $n_k(Q)$ of *all* compartments follow one by one. All we have to do is to apply the balance equation (4) iteratively, starting from the last compartment and working our way towards the first one, as follows:

$$\begin{aligned} n_{k-1}(Q) &= \sqrt{-\frac{1}{B_R} W(-B_R[n_k^2 e^{-B_L n_k^2} + Q])} \\ &= g(Q, n_k), \quad \text{for } k = K, \ldots, 3, 2, 1. \end{aligned} \tag{6}$$

This iterative mapping $n_{k-1}(Q) = g(Q, n_k)$ yields the steady flow profile along the whole length of the conveyor belt. The mapping is depicted in Fig. 5. The fixed point of the mapping, determined by $n_{k-1}(Q) = n_k(Q)$ or equivalently $g(Q, n_k) = n_k(Q)$, corresponds to a uniform profile along the whole system and will be denoted by $\tilde{n}(Q)$. This is the solution associated with the smooth flow of granular material at sufficiently small values of Q, as in Fig. 2(a). Only towards the end of the system there is an unavoidable departure from the uniform level $\tilde{n}(Q)$ because the profile has to link to the boundary condition of the last compartment Eq. (5).

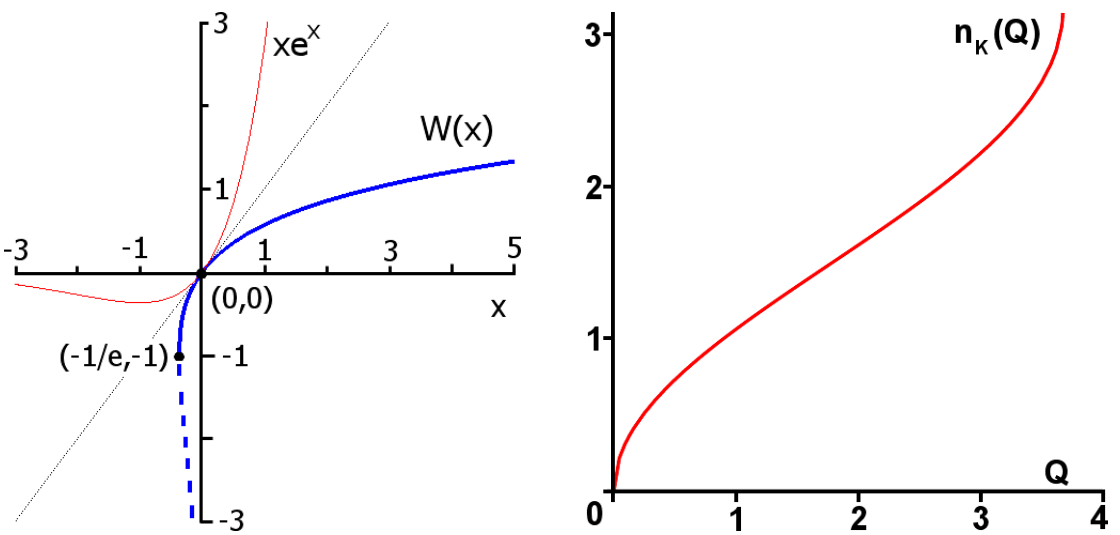

(a) (b)

Fig. 4. (a) The LambertW function $W(x)$ (heavy solid and dashed lines), defined as the solution of the equation $W(x)e^{W(x)} = x$, or equivalently, as the inverse of the function $f(x) = xe^x$ (thin red curve). The solution $n_K(Q)$ depicted in (b) corresponds to the small branch of $W(x)$ between the points $(0, 0)$ and $(-1/e, -1)$. The lower branch of $W(x)$ is dashed in order to emphasize that the LambertW function is double-valued on the interval $-1/e < x < 0$, so here one has to choose which branch corresponds to the problem at hand. (b) The density in the last compartment, $n_K(Q)$, as a function of the inflow rate Q. It is determined by the balance equation (5), with $B_R = 0.1$, which simply states that — under steady flow conditions — the outflow from the system must be equal to the inflow. Beyond $Q = 1.87372$ the flow becomes unstable and clustering sets in, so in practice the density of the last compartment is never observed to exceed the corresponding value $n_K(Q) = 1.54$. The only exceptions to this rule are found in extremely short transport lines consisting of just 1 or very few compartments (see Sec. 4.2). The maximum value of $n_K = 3.16228$ corresponds — naturally — to the density at which the flux function $F_R(n_k)$ attains its maximum, cf. Fig. 1(b).

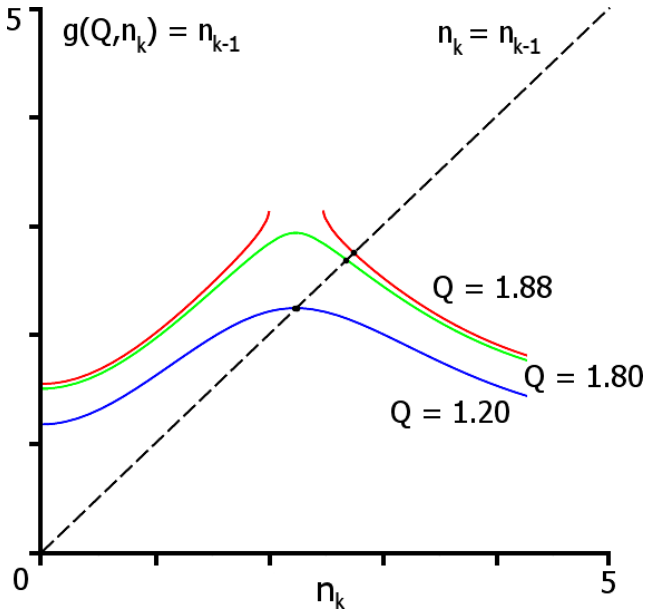

Fig. 5. The mapping $n_{k-1}(Q) = g(Q, n_k)$, given by Eq. (6), for three successive values of the inflow rate Q. The fixed point of the mapping — where the function $g(Q, n_k)$ intersects the diagonal, indicated by a solid dot — corresponds to a uniform profile along the conveyor belt. For $Q = 1.88$ the mapping shows a gap in the middle, which is a direct consequence of the fact that the LambertW function $W(x)$ is not defined for $x < -1/e = -0.37$ [see Fig. 4(a)].

The fixed point $\tilde{n}(Q)$ becomes unstable at $Q_{\rm bif} = 1.8878$ (close but not exactly equal to $Q_{\rm cr}$) by means of a reverse period doubling bifurcation. This happens when the slope of $g(Q, n_k)$ at the point $\tilde{n}(Q)$ becomes smaller (i.e. steeper) than -1. In this bifurcation, as we will show shortly, an unstable solution of periodicity 2 closes in upon $\tilde{n}(Q)$ and turns it unstable. It is precisely this period-2 solution that lies at the basis of the density oscillations with wavelength two compartments observed in the numerical experiments of the previous section.

Where does the period-2 solution come from? To answer this question, we turn to the twice-iterated map $n_{k-2}(Q) = g(g(Q, n_k))$, which is depicted in Fig. 6. It is seen that, at the value $Q = 1.855$, two new intersection points with the diagonal line come into existence. These points correspond to the two elements $n_a(Q)$ and $n_b(Q)$ of a period-2 solution. The old intersection point $\tilde{n}(Q)$, which is of period-1, is of course also a solution of the twice iterated map.

The stability of these solutions is determined by the derivative of the mapping. The stability criterion for the period-1 solution, as mentioned above, is

$$\left|\frac{dg(Q,n)}{dn}\right|_{n=\tilde{n}(Q)} < 1, \qquad (7)$$

which is satisfied for $0 < Q < 1.8878$. Likewise, the stability condition for the period-2 solution is (with $g^2(Q, n_k)$ denoting the twice iterated map $g(g(Q, n_k))$):

$$\left|\frac{dg^2(Q,n)}{dn}\right|_{n=n_a} = \left|\frac{dg^2(Q,n)}{dn}\right|_{n=n_b} < 1, \qquad (8)$$

which, however, is *never* satisfied. In Fig. 6 we see that — in order for the period-2 solution to exist — the slope of $g^2(Q, n_k)$ necessarily has to exceed unity at n_a and n_b, otherwise it would not intersect the diagonal. So the period-2 solution is always unstable. For increasing values of Q, its elements $n_a(Q)$ and $n_b(Q)$ close in upon the period-1 orbit $\tilde{n}(Q)$, and ultimately (at $Q = Q_{\rm bif} = 1.8878$) coincide with it. In the process, the basin of attraction of $\tilde{n}(Q)$ (bounded by the two elements of the period-2 orbit) vanishes.

This bifurcation is depicted in Fig. 7. In the same figure we also show how this gives rise to the oscillatory profile: If the value of Q is such that the density $n_{K-1}(Q)$ of the one-but-last compartment falls within the basin of attraction of $\tilde{n}(Q)$ (shaded area), all the successive densities $n_{K-2}(Q), n_{K-3}(Q), \ldots, n_1(Q)$ will oscillate towards the uniform solution $\tilde{n}(Q)$. This is the case for $Q < Q^* = 1.87346753$.

It should be noted that also in the case of a forward period-doubling bifurcation the event would be announced in advance by a similar oscillatory pattern. The main difference is that for a *reverse* bifurcation, as we have here, the critical value of Q at which the clustering sets in already occur (for any sizeable conveyor belt) *before* the bifurcation value $Q_{\rm bif}$. This has to do with the subcritical basin of attraction shown in Figs. 7 and 8, as we will discuss in the next subsection.

4.2. *The critical value $Q_{\rm cr}(K)$*

In the system at hand, the critical inflow rate beyond which clustering becomes inevitable is *not* the same as the bifurcation value $Q_{\rm bif}$. Moreover, it depends on the number of compartments K. For realistically sized conveyor belts (including the case with $K = 25$ compartments) the critical value $Q_{\rm cr}(K)$ is smaller than $Q_{\rm bif}$, while for very short

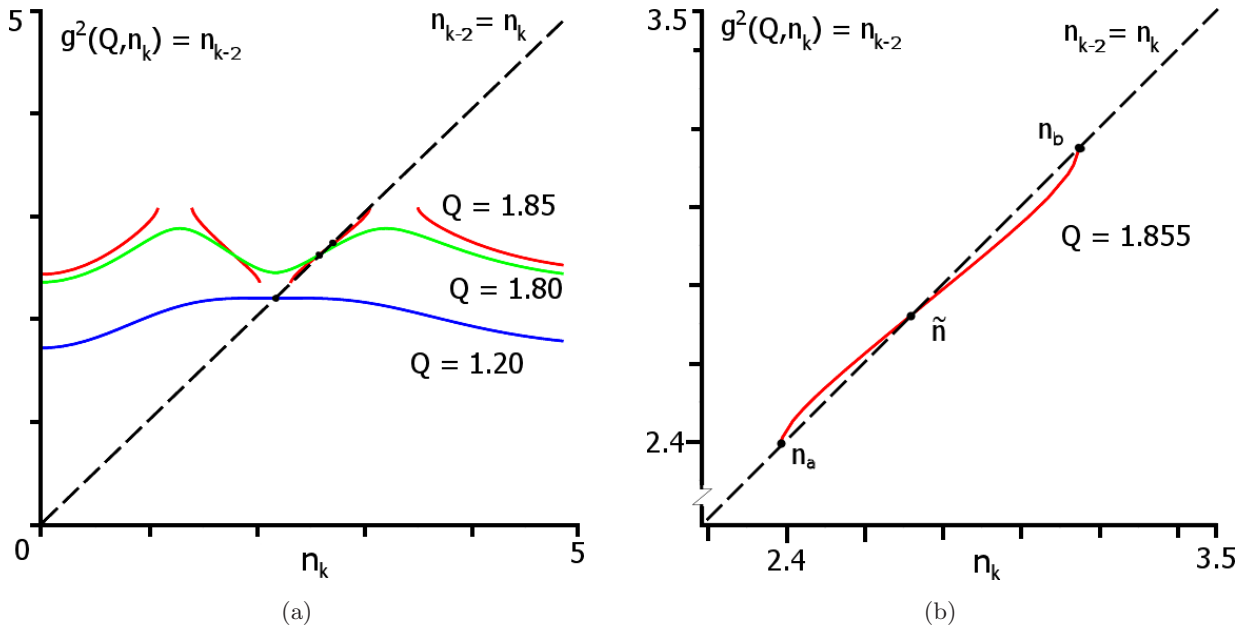

(a) (b)

Fig. 6. (a) The twice iterated mapping $g^2(Q, n_k) = g(g(Q, n_k))$ for three successive values of the inflow rate Q. The gaps in the mapping at $Q = 1.85$ are again a consequence of the fact that the LambertW function (which appears in the mapping) is not defined when its argument falls below $-1/e$; cf. Figs. 4(a) and 5. (b) Detailed view of the middle part of the same mapping, showing the two new points n_a and n_b, which together constitute an unstable orbit of period 2. The fixed point $\tilde{n}$ is present as well, since it satisfies the same period-2 condition $g^2(Q, n_k) = n_{k-2}$.

conveyor belts it is larger. Here we will explain this subtle point.

At $Q = Q^* = 1.87346753$ the density of the last-but-one compartment $n_{K-1}(Q)$ coincides with the boundary of the basin of attraction, i.e. with $n_a(Q)$ [see Fig. 8 and also Fig. 2(d)]. When this happens, the oscillation does no longer converge towards $\tilde{n}(Q)$. Instead, all the successive densities coincide alternatingly with $n_a(Q)$ and $n_b(Q)$, so in this case the oscillatory profile has a constant amplitude.

When the inflow rate is increased beyond Q^*, the density $n_{K-1}(Q)$ falls *outside* the basin of attraction of $\tilde{n}(Q)$: $n_{K-1}(Q) < n_a(Q)$. Consequently

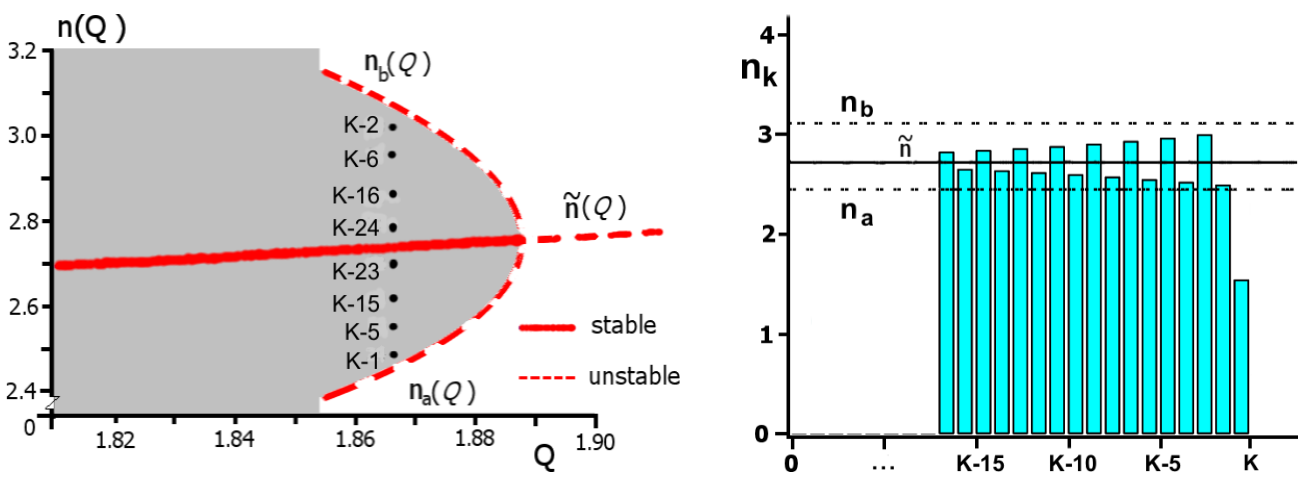

(a) (b)

Fig. 7. (a) The reverse period doubling bifurcation. The basin of attraction of the fixed point $\tilde{n}(Q)$ is indicated in gray; its boundaries are given (from $Q = 1.855$ onward) by the two elements of the unstable period-2 solution $n_a(Q)$ and $n_b(Q)$. The points $k = K-1, K-2, \ldots, K-23, K-24$ represent the densities in the successive compartments from right to left. (b) The density profile along the conveyor belt: The wavy profile is the result of the oscillatory convergence towards the fixed point $\tilde{n}(Q)$.

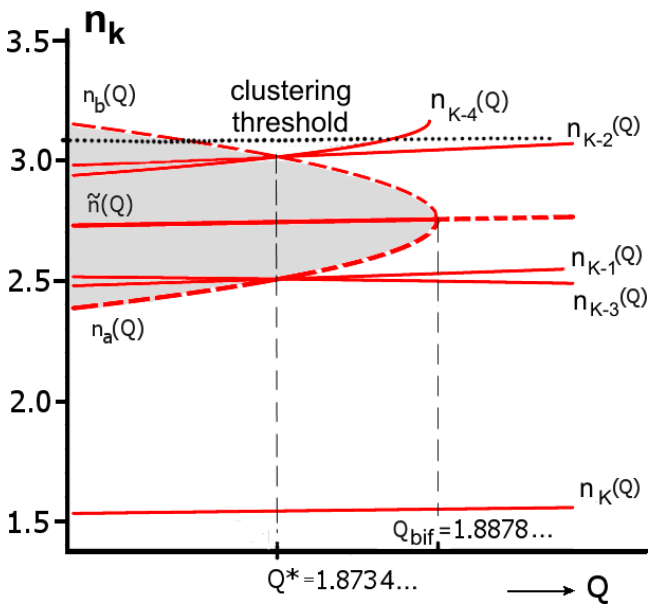

Fig. 8. The densities $n_k(Q)$ in the last five compartments $k = K, K-1, \ldots, K-4$. For $Q < Q^*$ all densities $n_{K-1}(Q), n_{K-2}(Q), \ldots$ fall inside the (shaded) basin of attraction of the fixed point $\tilde{n}(Q)$ and oscillate toward it, just as in Fig. 7. At $Q = Q^* = 1.87346753$ the density $n_{K-1}(Q)$ coincides with $n_a(Q)$ (and $n_{K-2}(Q)$ with $n_b(Q)$, and $n_{K-3}(Q)$ with $n_a(Q)$ again, etc.), hence for this particular Q-value the oscillatory profile has a constant amplitude along the entire system. For $Q > Q^*$ the densities fall *outside* the basin of attraction and progressively move away from the fixed point $\tilde{n}(Q)$. The horizontal dotted line at $n_k = 3.16228$ is the clustering threshold: When the density exceeds this line, clustering becomes inevitable.

the densities $n_{K-2}(Q), n_{K-3}(Q), \ldots, n_1(Q)$ move away from the fixed point $\tilde{n}(Q)$, despite the fact that this point is still stable until $Q_{\rm bif}$. So for $Q > Q^*$ the amplitude of the oscillation increases as we move to the left. If the conveyor belt is infinitely long ($K \to \infty$), this means that the amplitude sooner or later exceeds the threshold level $n_k = 3.16228$ beyond which clustering becomes inevitable[2]; in this case the critical inflow rate is simply equal to Q^*, i.e. $Q_{\rm cr}(\infty) = Q^* = 1.87346753$.

For a finite system on the other hand, in order for the densities to reach the threshold level $n_k = 3.16228$ a certain minimum growth rate of the amplitude is required. In this case the critical value $Q_{\rm cr}(K)$ must slightly exceed Q^*, and increasingly so as the number of compartments K becomes smaller. This is shown in Fig. 9. For instance, for $K = 25$ we find $Q_{\rm cr}(25) = 1.87372$ [cf. Figs. 2(e) and 3] and in the extreme case of $K = 1$ the critical inflow rate is $Q_{\rm cr}(1) = 3.67879$, almost *twice* as large as that for long conveyor belts.

This latter value can in fact be found analytically, because for the special case of $K = 1$ the leftmost compartment happens to be also the *last* compartment. So $Q_{\rm cr}(1)$ is simply the maximum Q-value for which the outflow from the last compartment can keep up with the inflow (irrespective of the mapping $g(Q, n_k)$ or its fixed point $\tilde{n}(Q)$, since these things come into play only for more than 1 compartment). This maximum Q-value can be read from Fig. 4, or determined analytically from the last-compartment condition $Q = F_R(n_K) = n_K^2 e^{-B_R n_K^2}$. So again the flux function to the right is

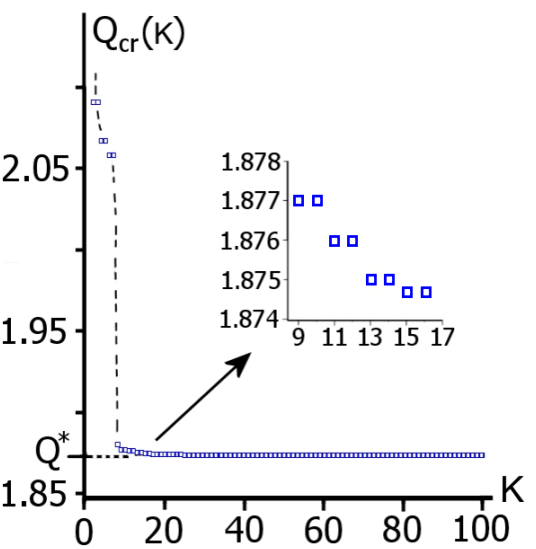

Fig. 9. The critical inflow rate $Q_{\rm cr}(K)$ as a function of the number of compartments K. The limit for $K \to \infty$ corresponds to the value $Q_{\rm cr}(\infty) = Q^* = 1.87346753$ of Fig. 8. Beyond this Q-value the densities fall outside the basin of attraction of $\tilde{n}(Q)$ and will oscillate away from it, which (given an infinitely long system) inevitably leads to clustering. The opposite limit for $K = 1$ (outside the scale of this figure, $Q_{\rm cr}(1) = (eB_R)^{-1} = 3.67879441$) corresponds to the maximum value of Q for which the outflow can equal the inflow. This is the Q-value associated with the rightmost point of the function $n_K(Q)$ in Fig. 4, with the annotation that for $K = 1$ the last compartment happens to be also the first one.

[2]The threshold level for clustering lies at $n_k = B_R^{-1/2} = 3.16228$, the density for which the flux function $F_R(n_k)$ is maximal. When n_k exceeds this value, the flux to the right will *diminish* with any further density increase. Given that the flux to the left has been a decreasing function of the density already from $n_k = B_L^{-1/2}$ onward, this means that clustering becomes unavoidable. Particles still stream into the compartment, but the outflow decreases further and further with every added particle.

the decisive limiting factor. This function attains its maximum when the derivative with respect to n_K vanishes, i.e. at $n_K = B_R^{-1/2} = 3.16228$ (for $B_R = 0.1$). The corresponding maximum value is $Q_{\rm cr}(1) = (eB_R)^{-1} = 3.67879$.

An interesting property, seen clearly in the inset of Fig. 9, is that $Q_{\rm cr}(K)$ depends on K pairwise. The reason for this that high densities — and hence the risk of cluster formation — only occur in every second compartment: If the cluster is destined to occur in the first compartment for a certain value of K, say 25, one may safely add an extra compartment in front of it (bringing the total number of compartments to 26) without harming the capacity of the conveyor belt, because this new compartment will have a relatively low density. The clustering in that case starts in compartment 2.

5. Discussion

5.1. *The explanation of the subcritical pattern formation*

As we have seen, the explanation of the oscillatory pattern lies in the fact that the uniform density level $\tilde{n}(Q)$ [i.e. the fixed point of the box-to-box mapping $n_{k-1} = g(Q, n_k)$] becomes unstable via a period-doubling bifurcation. This induces, in an interval of Q-values before the actual destabilization takes place [from the birth of the unstable period 2-solution until $Q_{\rm cr}(K)$], an oscillatory convergence towards $\tilde{n}(Q)$. It is precisely this oscillation with its spatial periodicity of two compartments that constitutes the subcritical pattern.

We have also demonstrated that the critical inflow rate $Q_{\rm cr}(K)$ is governed by the combined action of the last-compartment condition Eq. (5) [which determines the density of the last-but-one compartment $n_{K-1}(Q)$], the reverse period-2 solution [which constitutes the borders of the basin of attraction of $\tilde{n}(Q)$] and a finite-size effect: For $K \to \infty$ the critical value is equal to Q^*, i.e. the Q-value at which $n_{K-1}(Q)$ coincides with an element of the period-2 solution. For finite K the critical value exceeds Q^* as depicted in Fig. 9.

5.2. *On the robustness of the oscillatory pattern*

In the introduction, we have already mentioned that the oscillatory density profile is of significant potential interest for industries that handle granular materials, where it could be exploited as a warning signal for imminent cluster formation. Naturally, the practical value of the phenomenon greatly depends on its robustness. Does it survive in the presence of noise? And how sensitively does it depend on the form of the flux function? Let us briefly discuss these important questions.

To get insight into the robustness with respect to noise, we add a fluctuating part to the flow between the boxes. That is, the flux from box k *on average* still follows the behavior dictated by $F_{R,L}(n_k)$, but there may always be a few stray particles that make it either smaller or larger. We can model this via the following modified flux function:

$$\tilde{F}_{R,L}(n_k) = (1 + \lambda \cdot {\rm rand}_{k(R,L)}) F_{R,L}(n_k), \qquad (9)$$

where λ determines the relative strength of the fluctuations and ${\rm rand}_{k(R,L)}$ denotes a set of random numbers. These numbers are picked anew at each time step of the numeric integration procedure (two for each compartment, one for the flux to the right and one for the left) from a normal distribution with mean value $\mu = 0$ and variance $\sigma^2 = 1/2\pi = 0.159$, i.e.

$$f_{\mu,\sigma}(r) = \frac{1}{\sigma\sqrt{2\pi}} e^{-(r-\mu)^2/2\sigma^2} = e^{-\pi r^2}. \qquad (10)$$

Figures 10 and 11 show the results for $\lambda = 0.01$ (a relative noise level of 1%) and $\lambda = 0.05$ (5%), respectively. The inflow rate in both cases is $Q = 1.87$, just below the critical value $Q_{\rm cr}(25) = 1.87372$ for the same 25-compartment system in the absence of noise ($\lambda = 0$). In Fig. 10, we observe that the fluctuations make the oscillatory profile less regular, as expected, but do not yet succeed in tipping the scale toward clustering. In Fig. 11, with its fivefold noise level, they *do* succeed in doing so.

Interestingly, the clustering in the presence of noise does not necessarily start in the leftmost compartment. In the numerical experiment of Fig. 11 the first clusters happen to originate in compartments 23 and 9. Slowly but inevitably, however, as these clusters obstruct the flow and induce the formation of new clusters toward the left, the leftmost compartments start to dominate. At $\tau = 200$ the newly formed cluster in compartment 2 is already about five times as big as the other two.

The most important point for the present purposes, however, is the fact that even at these high noise levels the oscillatory pattern is seen to survive for some time. Therefore, it can still be used as a warning signal: If direct measures are taken

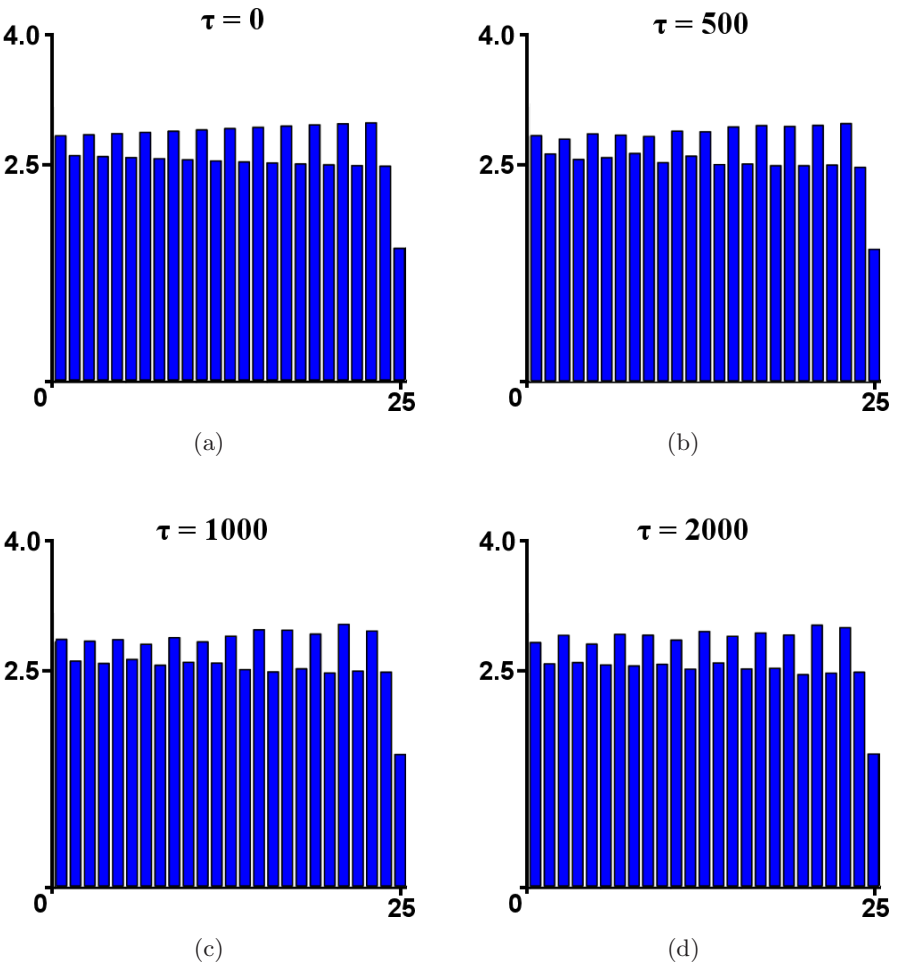

Fig. 10. Evolution of the density profile for $Q = 1.87$ if the flux function fluctuates randomly [as in Eq. (9)] with $\lambda = 0.01$. As initial condition at $\tau = 0$ we have taken the density profile for the same Q-value in the absence of noise, cf. Fig. 2(c). The oscillatory profile survives without any appreciable loss of amplitude, only somewhat less regular.

(in Fig. 11 one might postpone it until $\tau = 20$, but not much longer) the clustering may still be avoided.

In order to test the robustness of the oscillations with respect to the precise form of the flux function, we will try various forms of $F_{R,L}(n_k)$. However, not just any form will do. We recall that the flux function must obey certain general rules: It should be zero at $n_k = 0$, then attain a maximum (at some finite value of n_k) and finally go to zero again for $n_k \to \infty$. With this in mind, let us consider the following *family* of flux functions [see Fig. 12(a)]:

$$F_{R,L}(n_k) = A n_k^{\alpha} e^{-B_{R,L} n_k^2}, \tag{11}$$

where the power α is not necessarily equal to 2 (as in the rest of the paper) but may in principle be any positive number. Not every value of α is equally realistic, of course, but values between 1 and 2 make good sense.

The flux function with $\alpha = 2$ was derived on the basis of granular hydrodynamics under the assumption that the energy losses in the granular medium are entirely due to the binary collisions of the particles between themselves [Eggers, 1999]. The dissipative effect due to the collisions with the walls is neglected. This is a reasonable approximation when the density of the particles is large. At low densities, however, the collisions with the walls will be the dominant factor and the number of these collisions per unit time does not depend on the density as n_k^2 but as n_k. From this, it may be inferred that in the low-density regime the flux function should grow linearly rather than quadratically with n_k, supporting the choice $\alpha = 1$ [Van der Weele, 2008]. Also an intermediate value $1 < \alpha < 2$ is a realistic option. Indeed, experiments [Jean *et al.*, 2002; Leconte & Evesque, 2006; Evesque, 2007] and direct simulations of the granular flow from a compartment [Mikkelsen *et al.*, 2005] show a less-than-quadratic

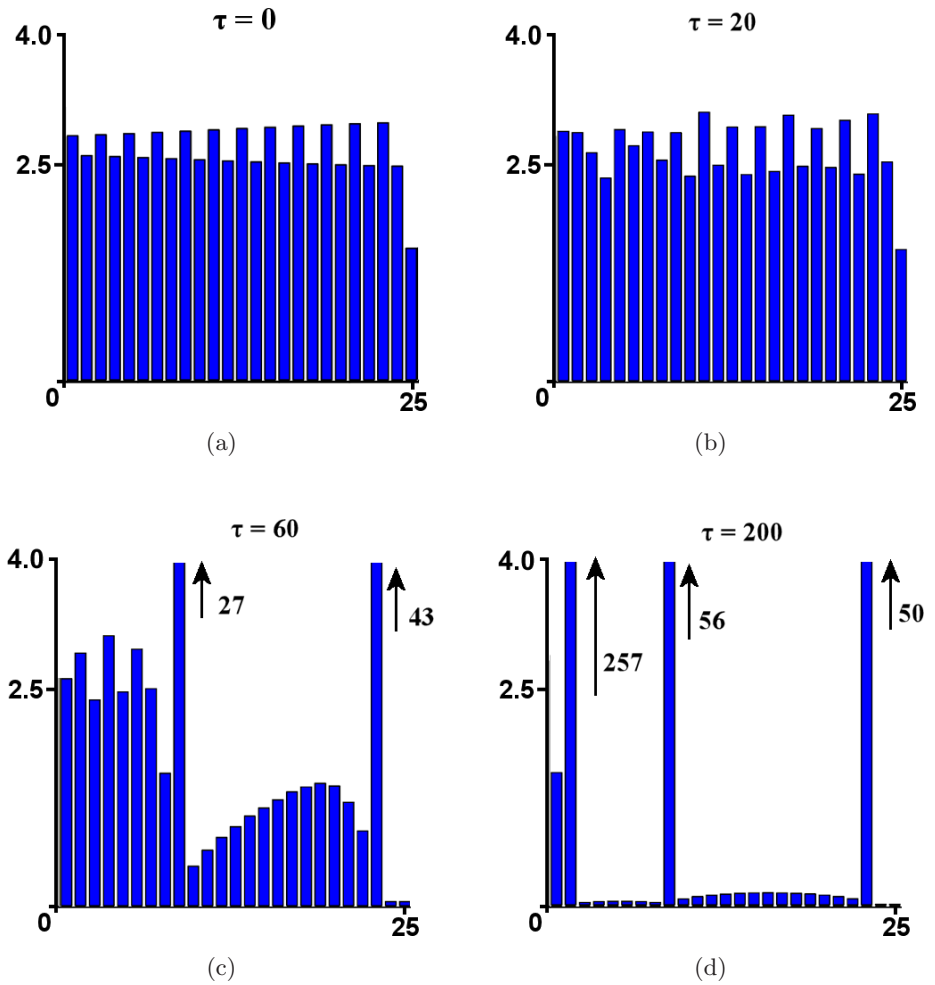

Fig. 11. Evolution of the density profile for $Q = 1.87$ with a flux function that fluctuates randomly [as in Eq. (9)] with $\lambda = 0.05$. The initial condition is the same as in Fig. 10, but due to the larger amplitude of the fluctuations (five times as large as in Fig. 10) the density in several compartments soon exceeds the critical level and clustering sets in. Nevertheless, up to $\tau = 20$ the oscillatory profile is clearly recognizable and provides a meaningful warning signal for the imminent clustering.

but not purely linear dependence.[3] We will therefore also consider the case $\alpha = 1.5$ as a typical example.

Figures 12(b)–12(d) show the critical profiles, at the brink of clustering, for $\alpha = 1$, $\alpha = 1.5$ and $\alpha = 2$ [the latter profile is the same as in Fig. 2(e)]. It is seen that the maximum capacity of the system, i.e. the value of the critical flow rate $Q_{\rm cr}(25)$, differs drastically between the three flux functions. This does not come as a surprise, of course, given the fact that the maximum of $F_R(n_k)$ [depicted in Fig. 12(a)] for $\alpha = 1$ is only $A(2B_Re)^{-1/2} = 1.36$ per dimensionless time unit, whereas the maximum for $\alpha = 2$ is $A(B_Re)^{-1} = 3.68$. The capacity of the latter is therefore much larger. Also other characteristics change with the value of α, such as the slope of the density profile near the final compartment and — associated with this — the precise positioning of the maxima and minima along the conveyor belt. For instance, for $\alpha = 1$ the density has a *minimum* in the first compartment whereas for $\alpha = 2$ (and also for $\alpha = 1.5$) it has a maximum. Nevertheless, despite all these changes, the oscillatory pattern is preserved.

All in all, we may conclude that the subcritical oscillatory density profile is quite a robust feature for these types of flow.

[3]The experimental studies also show that the shape of the flux function (especially around the maximum and in the tail) alters as a function of the driving frequency; and via a bifurcation-theoretical analysis the authors predict that this must have a marked influence on whether the clustering transition is super- or sub-critical [Leconte & Evesque, 2006; Evesque, 2007]. This feature is not captured by the present family of flux functions.

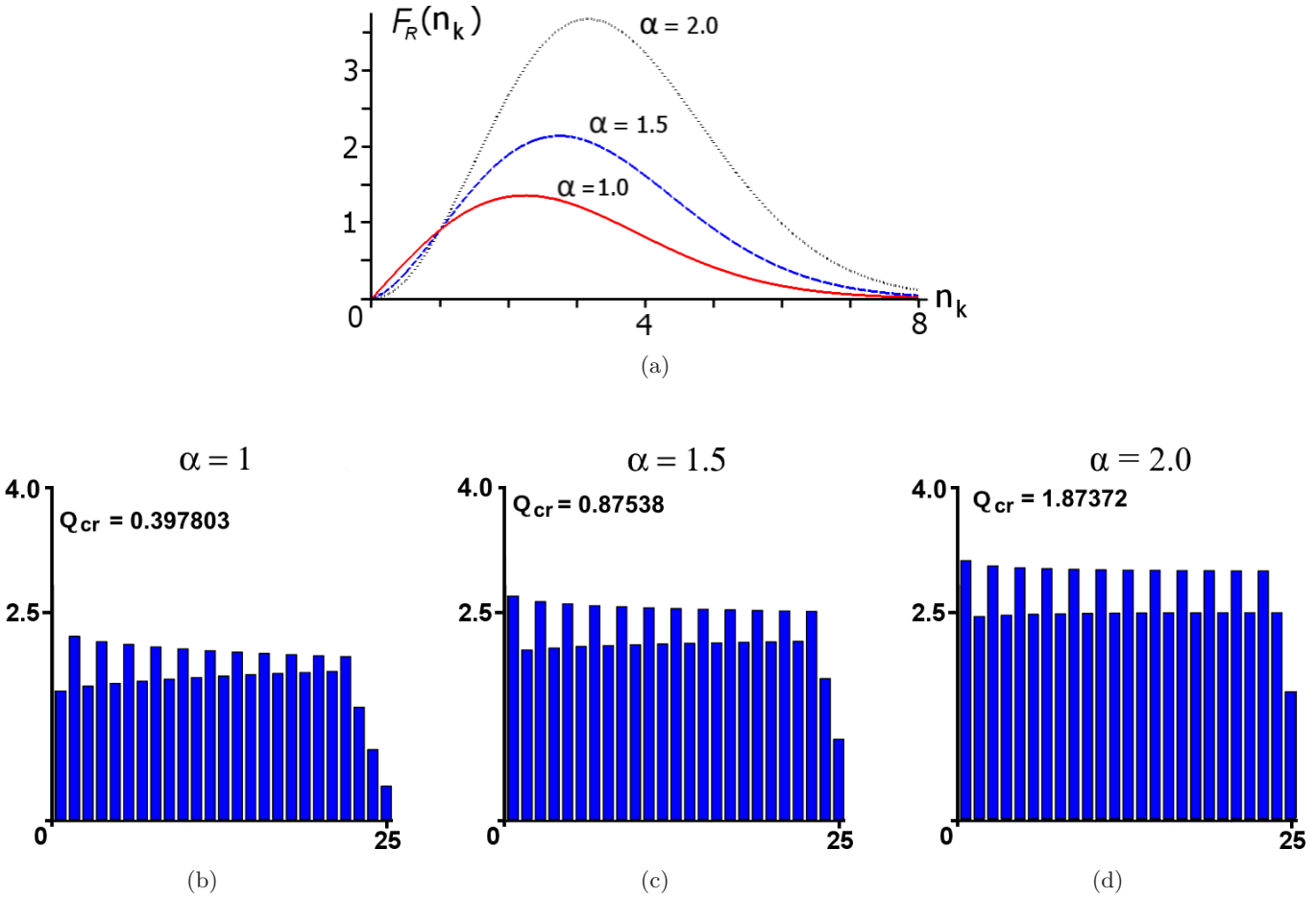

Fig. 12. (a) Three different members of the family of flux functions $F_R(n_k)$ defined by Eq. (11), here depicted for $A = 1$ and $B_R = 0.1$, with the power α respectively equal to 1, 1.5 and 2. The one for $\alpha = 2$ is the Eggers flux function Eq. (1) that has been used throughout the paper. (b)–(d) The associated critical flow patterns. Changing the value of α has a pronounced influence on the maximum capacity of the system (expressed by $Q_{\rm cr}$) and also alters the slope of the density profile near the rightmost compartment. The characteristic oscillatory pattern, however, is seen to be preserved.

5.3. *Further directions*

The appearance of oscillations in the density profile is, as stated in the introduction, a clear-cut example of spontaneous pattern formation. As such it may serve as a basis for the study of many related phenomena in out-of-equilibrium transport systems. The transport need not be restricted to material flows but may also concern the flow of energy or momentum. One instance of particular interest is the energy cascade in turbulent fluids.

As is well known, the energy in three-dimensional turbulence is transported from the large length scales to the smaller ones. One of the models that has been put forward to describe this is the GOY model, named after Gledzer, Ohkitani and Yamada [Gledzer, 1973; Yamada & Ohkitani, 1987, 1988; Ohkitani & Yamada, 1989]. In this model the spectrum of relevant length scales is divided into N discrete shells, with the first shell representing the largest and the Nth shell the smallest length scale. To be specific, the nth shell is determined by a wave number $k_n = k_0\lambda^n$ with $\lambda > 1$ $(n = 1, 2, \ldots, N)$. Each shell is characterized by a complex velocity mode u_n, which is coupled to the modes in the nearest and next nearest shells in a way that mimics the underlying hydrodynamic equations.

Energy is being put into the system in one of the first shells, and this energy is transferred to the next shells (higher n, smaller length scale) in a way similar to the granular transport studied in the present paper. In dynamic equilibrium all shells contain a certain energy $(1/2)|u_n|^2$, which is distributed in such a way that the product $u_n k_n^{1/3}$ oscillates around a constant level along most of the cascade [Schörghofer *et al.*, 1995; Kadanoff *et al.*, 1997]. The oscillatory profile of $u_n k_n^{1/3}$ is very

reminiscent[4] of that of Fig. 12, with only one intriguing difference, namely the periodicity of the oscillations is 3 instead of 2.

This period-3 pattern suggests that the oscillatory profile does not always have to be related to a period-doubling bifurcation but that also period-tripling is possible. And in other systems it may well occur via period-quadrupling (giving rise to a pattern with periodicity 4) or even higher periods. We hope to come back to this in a future publication.

Acknowledgments

We gladly seize the opportunity to congratulate Prof. Tassos Bountis on the occasion of his 60th birthday. He has been a friend and source of inspiration to us for as long as we remember, and our wish is that he will continue to be so — always in good spirits and good health — for many years to come! In the context of the present paper we thank Tassos Bountis, Marcel Kloosterman, Detlef Lohse, Devaraj van der Meer, and Christos Tsiavos for stimulating discussions and insightful remarks. This work is financially supported by the Carathéodory Programme (grant C167) of the University of Patras, Greece. It is part of the research programme of the European Complexity-NET project "Complex Matter".

References

Corless, R. M., Gonnet, G. H., Hare, D. E. G., Jeffrey, D. J. & Knuth, D. E. [1996] "On the Lambert W function," *Adv. Comput. Math.* **5**, 329–359.

Cross, M. C. & Hohenberg, P. C. [1993] "Pattern formation outside of equilibrium," *Rev. Mod. Phys.* **65**, 851–1112.

Eggers, J. [1999] "Sand as Maxwell's demon," *Phys. Rev. Lett.* **83**, 5322–5325.

Evesque, P. [1992] "Shaking dry powders and grains," *Contemp. Phys.* **33**, 245–261.

Evesque, P. [2007] "How one can make the bifurcation of Maxwell's demon in granular gas hyper-critical," *Poudres & Grains* **16**, 1–13.

Gledzer, E. B. [1973] "System of hydrodynamic type admitting two quadratic integrals of motion," *Sov. Phys. Dokl.* **18**, 216–217; English translation [1973] *Dokl. Akad. Nauk SSSR* **209**, 1046–1048.

Goldhirsch, I. & Zanetti, G. [1993] "Clustering instability in dissipative systems," *Phys. Rev. Lett.* **70**, 1619–1622.

Jaeger, H., Nagel, S. & Behringer, R. [1996] "Granular solids, liquids, and gases," *Rev. Mod. Phys.* **68**, 1259–1273.

Jean, P., Bellenger, H., Burban, P., Ponson, L. & Evesque, P. [2002] "Phase transition or Maxwell's demon in granular gas?" *Poudres & Grains* **13**, 27–39.

Kadanoff, L., Lohse, D. & Schörghofer, N. [1997] "Scaling and linear response in the GOY turbulence model," *Physica D* **100**, 165–186.

Kanellopoulos, G. & Van der Weele, K. [2008] "Critical flow of granular matter on a conveyor belt," *Let's Face Chaos Through Nonlinear Dynamics*, eds. Robnik, M. & Romanovski, V., *AIP Conf. Proc.*, Vol. 1076, pp. 112–121.

Kudrolli, A., Wolpert, M. & Gollub, J. P. [1997] "Cluster formation due to collisions in granular material," *Phys. Rev. Lett.* **78**, 1383–1386.

Leconte, M. & Evesque, P. [2006] "Maxwell demon in granular gas: A new kind of bifurcation? The hypercritical bifurcation," arXiv:physics/0609204v1, 25 September 2006.

Mikkelsen, R., Van der Weele, K., Van der Meer, D., Van Hecke, M. & Lohse, D. [2005] "Small-number statistics near the clustering transition in a compartmentalized granular gas," *Phys. Rev. E* **71**, 041302-1–041302-12.

Ohkitani, K. & Yamada, M. [1989] "Temporal intermittency in the energy cascade process and local Lyapunov analysis in fully-developed model turbulence," *Prog. Theor. Phys.* **81**, 329–341.

Schörghofer, N., Kadanoff, L. & Lohse, D. [1995] "How the viscous subrange determines inertial range properties in turbulence shell models," *Physica D* **88**, 40–54.

Van der Meer, D., Van der Weele, K., Reimann, P. & Lohse, D. [2007] "Compartmentalized granular gases: Flux model results," *J. Stat. Mech.: Th. Exper.* **2007**, P07021-1–P07021-28.

Van der Weele, K., Van der Meer, D., Versluis, M. & Lohse, D. [2001] "Hysteretic clustering in granular gas," *Europhys. Lett.* **53**, 328–334.

Van der Weele, K., Mikkelsen, R., Van der Meer, D. & Lohse, D. [2004] "Cluster formation in compartmentalized granular gases," *The Physics of Granular*

[4]The similarity is made even more striking by the fact that the profile of $u_n k_n^{1/3}$ falls off rapidly (and vanishes) at the high-n end of the cascade, known as the Kolmogorov scale, where the turbulent motion is damped out by viscous effects. A careful stability analysis of the period-3 solution, which may be interpreted as the counterpart of our last-compartment condition Eq. (5), reveals the way in which this decay happens [Kadanoff *et al.*, 1997].

Media, eds. Hinrichsen, H. & Wolf, D. (Wiley-VCH, Weinheim, Germany), pp. 117–139.

Van der Weele, K. [2008] "Granular gas dynamics: How Maxwell's demon rules in a non-equilibrium system," *Contemp. Phys.* **49**, 157–178.

Van der Weele, K., Kanellopoulos, G., Tsiavos, Ch. & Van der Meer, D. [2009] "Transient granular shock waves and upstream motion on a staircase," *Phys. Rev. E* **80**, 011305-1–011305-16.

Yamada, M. & Ohkitani, K. [1987] "Lyapunov spectrum of a chaotic model of three-dimensional turbulence," *J. Phys. Soc. Jpn.* **56**, 4210–4213.

Yamada, M. & Ohkitani, K. [1988] "The inertial subrange and non-positive Lyapunov exponents in fully-developed turbulence," *Prog. Theor. Phys.* **79**, 1265–1268.